Green Chemistry

PAPER

View Article Online
View Journal | View Issue

Cite this: *Green Chem.*, 2014, **16**, 4162

Gold supported on titania for specific monohydrogenation of dinitroaromatics in the liquid phase†

Shuang-Shuang Liu, Xiang Liu, Lei Yu, Yong-Mei Liu,* He-Yong He and Yong Cao*

Received 13th May 2014,
Accepted 25th June 2014

DOI: 10.1039/c4gc00869c

www.rsc.org/greenchem

Liquid-phase selective monohydrogenation of various substituted dinitroaromatics to the corresponding valuable nitroanilines was investigated on gold-based catalysts. Special attention was paid to the effect of Au particle size on this monoreduction reaction. Interestingly, TiO_2 supported gold catalysts containing a relatively larger mean Au particle size (>5 nm) showed far superior chemoselectivity for specific monohydrogenation of dinitroaromatics, with the highest performance attainable for the catalyst bearing Au particles of *ca.* 7.5 nm. Results in the intermolecular competitive hydrogenation showed that the intrinsic higher accumulation rates of the desired nitroanilines associated with the catalyst possessing larger Au particles were responsible for the high chemoselectivity observed.

Introduction

Nitroanilines represent an attractive target for organic synthesis and are important intermediates for dyes, pharmaceuticals and agrochemicals because of their inherently reactive nature as highly versatile synthons.[1] Despite many known methods, there is ongoing interest in the development of convenient and general protocols for the synthesis of these compounds. Hence, in recent years, novel approaches such as palladium-catalyzed one-pot conversion of nitro compounds with silanes[2] and ammonolysis of nitrobenzenes[3] have been developed. In spite of all these achievements, the selective monoreduction of readily available dinitroaromatics represents the most straightforward and efficient route to this class of compounds.[4] Known reductions of dinitroaromatics make use of stoichiometric amounts of sulfide reagents or iron powder.[5] Recently, some homogeneous as well as heterogeneous catalytic systems in combination with different hydrogen donors have been developed.[6] The most ideal reductant for this purpose is molecular hydrogen (H_2), because, theoretically, water is the only by-product.[7] Although there are a few successful reports on the selective monoreduction of dinitroaromatics using H_2,[8] the applied catalytic metals such as palladium and ruthenium are flammable when exposed to air, and, in many cases, special handling is required. Thus, the development of a new, efficient and non-pyrophoric catalytic system capable of highly selective monohydrogenation of dinitroaromatics under mild, practical and convenient conditions is highly desired.

In recent years, catalysts based on supported gold nanoparticles (NPs) have attracted considerable attention as new promising nitro hydrogenation materials owing to their high intrinsic selectivity toward the formation of the desired amino compounds.[9] This was prompted by Corma's discovery of exceptionally high selectivity of TiO_2 supported gold NPs for the hydrogenation of nitroaromatics in the presence of other reducible functional groups.[10] We have recently contributed to the field of Au-catalyzed nitro reductions by discovering that the use of CO/H_2O or ammonium formate as a reducing agent can facilitate more efficient chemoselective nitro reduction under much milder conditions.[11] Whereas currently much attention has been focused on new improved protocols for selective nitro reduction, reports on the use of Au for the monoreduction of dinitroaromatics are scarce. In a precedent related to this work, Keane and co-workers have shown that monoreduction of dinitroaromatics under a gas phase H_2 atmosphere is possible over Au supported on Al_2O_3 or TiO_2, but an elevated temperature (commonly >200 °C) is required.[8e,f] This is not favourable for the synthesis of complex, thermolabile N-containing compounds typical in fine chemistry. A sustainable and industrially friendly low temperature process for the highly selective monohydrogenation of dinitroaromatics is thus of great fundamental as well as practical interest.

With our ongoing interest in selective nitro reduction catalyzed by a heterogeneous catalyst, we herein describe the unique catalytic behaviour of supported Au catalysts in the liquid phase mono-hydrogenation of dinitroaromatics. We

Shanghai Key Laboratory of Molecular Catalysis and Innovative Materials, Department of Chemistry, Fudan University, Shanghai 200433, P. R. China. E-mail: yongcao@fudan.edu.cn, ymliu@fudan.edu.cn; Fax: (+86-21) 65643774

† Electronic supplementary information (ESI) available: Experimental data, TEM, ^1H and ^{13}C NMR data. See DOI: 10.1039/c4gc00869c

demonstrate for the first time that, by fine tuning the particle size of Au NPs deposited on an inorganic support such as TiO_2, it is possible to obtain valuable nitroanilines in high yields *via* selective monohydrogenation of the corresponding dinitroaromatics under mild conditions. In contrast to the trends identified in the traditional Au-based nitro hydrogenation systems,[12] we have found that catalysts containing a relatively larger mean particle size (>5 nm) showed higher efficacy in the selective monoreduction of dinitroaromatics than catalysts containing a smaller particle size (<5 nm). Notably, the use of TiO_2-supported 7.5 nm gold NPs (Au-7.5/TiO_2) turned out to be the most effective catalyst for high-yielding monoreduction of a diversity of dinitroaromatics to nitroanilines. The catalytic system presented here, in which fine tuning of the product composition can be achieved by simply varying the Au particle size, may contribute to the design of new efficient and green catalytic systems for clean synthesis of nitroanilines and related derivatives under mild and convenient conditions.

Results and discussion

Synthesis and characterization

Two general methods were employed for the synthesis of a series of TiO_2 supported Au NPs with different mean diameters (Au-*x*/TiO_2, where *x* denotes the average particle size (nm) of metallic Au species): for the sample with a Au size smaller than 3 nm, a routine NaOH deposition–precipitation (DP) procedure was used (method A), whereas for the sample containing Au NPs with a size larger than 3 nm, a colloidal deposition approach[13] was employed (method B). Table 1 reports the gold loading in the catalysts determined by ICP-AES, as well as the other main characteristics of these catalysts. Note that the gold loading of the DP-derived samples is consistently lower than that obtained by method B, indicating that the latter is more efficient in terms of depositing Au particles onto the support. Fig. 1 shows the X-ray diffraction (XRD) patterns of the as-prepared Au-*x*/TiO_2 catalysts. It may be noted here that compared with the XRD patterns of the parent support material, the addition of Au produced no structural changes in the TiO_2 phases. Meanwhile, no diffraction lines of metal gold were observed for these Au-based catalysts.

Transmission electron microscopy (TEM) measurements were then carried out to identify the possible structures of the five different samples. As illustrated in Fig. 2, the Au NPs are all narrowly distributed and were varied in the range from 1.8 to 10 nm. X-ray photoelectron spectroscopy (XPS) was used to probe the oxidation state(s) of gold deposited on the surface of the TiO_2 support (Fig. 3). All samples showed features at 83.8 eV and 87.3 eV in a 4 : 3 peak area ratio, which were readily assigned to the $4f_{7/2}$ and Au $4f_{5/2}$ peaks, respectively, of metallic gold (*i.e.* Au^0). Additional information on the surface electronic states can be obtained from UV-Vis diffuse reflectance measurements.[14] As depicted in Fig. 4, the Au-*x*/TiO_2 catalysts exhibit a band with the peak in the wavelength range of 500–600 nm. This band is due to the surface plasmon resonance of the metallic Au NPs and is affected by the morphology of gold particles and the dielectric properties of the chemical environment.[15] At this point it is interesting to mention that there is a distinct shift in the peak maximum to longer wavelengths as the Au particle size increases.[16]

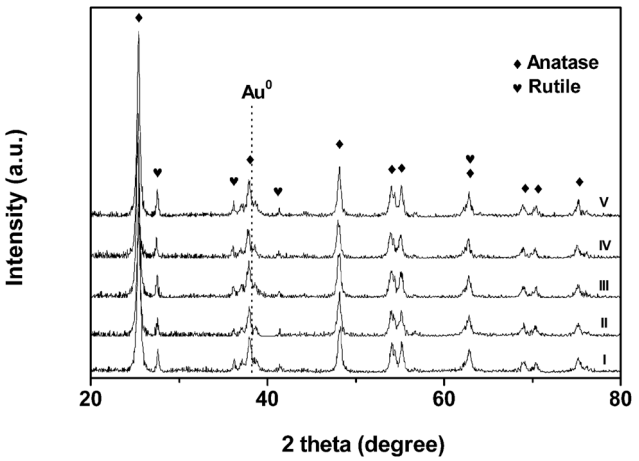

Fig. 1 XRD diffractograms: (I) Au-1.8/TiO_2, (II) Au-3.9/TiO_2, (III) Au-5.8/TiO_2, (IV) Au-7.5/TiO_2, and (V) Au-9.3/TiO_2.

Table 1 Main characteristics of the as-synthesized Au/TiO_2 catalysts

Catalyst	Au[a] (wt%)	UV-vis A_{max} (nm)	BET ($m^2\ g^{-1}$)	DP[b] (nm)
Au-1.8/TiO_2	0.56	559	48	1.8
Au-3.9/TiO_2	0.94	564	41	3.9
Au-5.8/TiO_2	0.95	570	39	5.8
Au-7.5/TiO_2	0.92	579	40	7.5
Au-9.3/TiO_2	0.94	582	37	9.3

[a] Based on ICP-AES analysis. [b] Based on TEM analysis.

Catalytic performance

Following most of the previous work on dinitroaromatic reduction reactions,[8] we also selected the *m*-dinitrobenzene (*m*-DNB) used as a model substrate. The problem of this particular transformation is the large variety of reduction products that can possibly be formed (Scheme 1). Besides *m*-nitroaniline (*m*-NA), *m*-phenylenediamine (*m*-PDA), azo and azoxy intermediates are also typical products formed in the monoreduction.[17] The target is to develop a selective process for the transformation of *m*-DNB into *m*-NA avoiding deep hydrogenation to *m*-PDA. In the preliminary study focused on the nature of the underlying support on the performance of a variety of supported Au NPs, the conversion of *m*-DNB was kept below 50% and observation of various reduction products derived from the reaction with various supported catalysts under 3 MPa H_2 at 60 °C is summarized in Table 2. Among the series of catalysts tested, the best performing catalyst was the benchmark titania supported Au catalyst Au-M/TiO_2 (average gold particle size ~2.8 nm, supplied by Mintek), which favoured the formation of *m*-NA with the selectivity of 64% at 48% *m*-DNB conversion (Table 2, entry 1), and only traces of

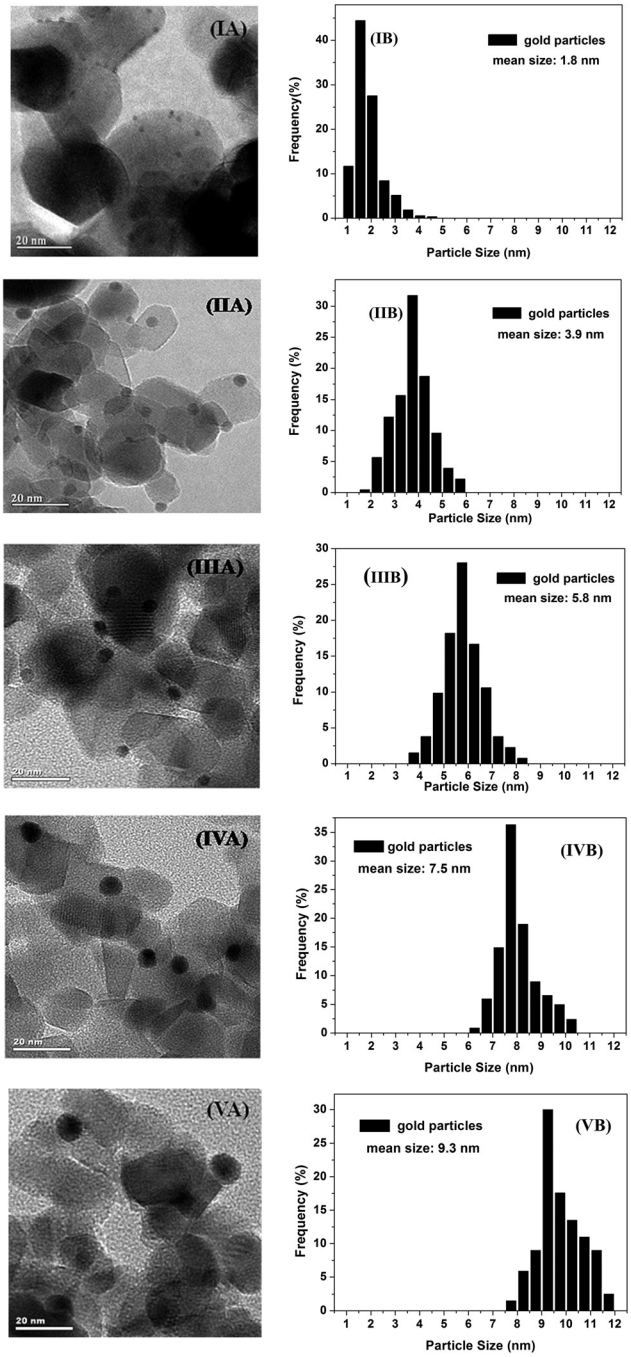

Fig. 2 Representative (A) TEM images and (B) Au particle size distributions of (I) Au-1.8/TiO_2, (II) Au-3.9/TiO_2, (III) Au-5.8/TiO_2, (IV) Au-7.5/TiO_2, and (V) Au-9.3/TiO_2 respectively.

azo and azoxy intermediates were generated. While gold with similar average particle size (*ca.* 3 nm, see Table S1†) supported on other supports, such as Au/CeO_2, Au/ZnO, Au/Al_2O_3, and Au/ZrO_2, also exhibited an appreciable activity for reduction of *m*-DNB, the formation of highly toxic azo and azoxy-derivatives represent the main drawbacks. Moreover, it should be noted that previously reported catalytic metals, such as Pt, Pd, and Ru, showed good activity but much inferior selectivity in terms of *m*-NA formation relative to Au under the

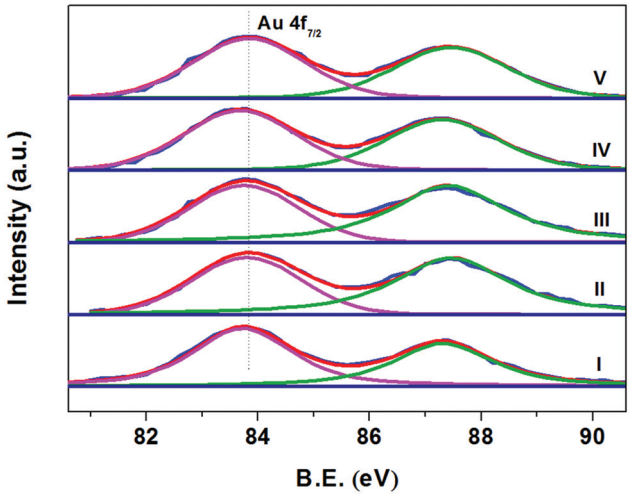

Fig. 3 XP spectra of the Au (4f) signal for Au/TiO_2: (I) Au-1.8/TiO_2, (II) Au-3.9/TiO_2, (III) Au-5.8/TiO_2, (IV) Au-7.5/TiO_2, and (V) Au-9.3/TiO_2.

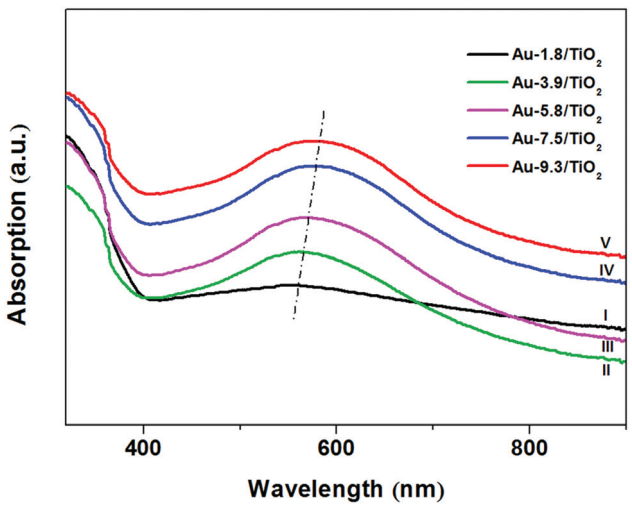

Fig. 4 UV-vis spectra of (I) Au-1.8/TiO_2, (II) Au-3.9/TiO_2, (III) Au-5.8/TiO_2, (IV) Au-7.5/TiO_2, and (V) Au-9.3/TiO_2.

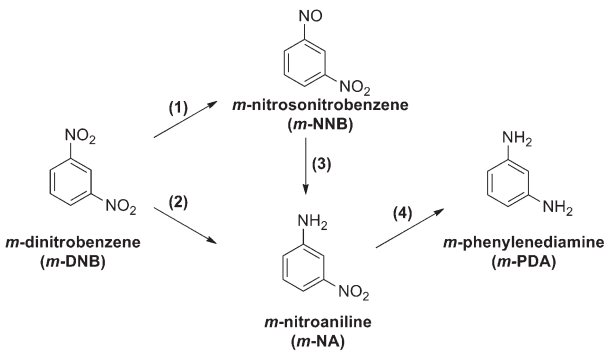

Scheme 1 Simplified pathway for hydrogenation of *m*-DNB.

Table 2 Liquid phase reduction of *m*-DNB to *m*-NA with H_2 in the presence of various catalysts[a]

Entry	Catalyst	*T* [min]	Conv.[b] [%]	Sel.[b] [%]				
				m-NA	*m*-PDA	*m*-NNB	Azo[c]	Azoxy[c]
1	Au/TiO_2	25	48	64	18	16	<1	<1
2	Au/ZnO	30	32	22	0	9	8	61
3	Au/Al_2O_3	20	50	40	5	16	9	30
4	Au/Fe_2O_3	30	6	66	0	19	6	9
5	Au/CeO_2	30	28	1	0	1	6	92
6	Au/ZrO_2	30	48	51	1	20	4	25
7	Au/SiO_2	30	11	65	1	13	9	12
8	Au/C	30	n.r.	—	—	—	—	—
9	TiO_2	30	n.r.	—	—	—	—	—
10	Pt/TiO_2	15	45	35	52	2	4	7
11	Pd/TiO_2	20	40	34	49	2	5	10
12	Ru/TiO_2	25	47	45	32	5	7	11

[a] Reaction conditions: 0.5 mmol *m*-DNB, metal: 0.5 mol%, 5 mL ethanol, 3 MPa H_2, 60 °C. n.r. = no reaction. [b] Conversion and selectivity determined by GC. [c] Azo stands for azo intermediate; azoxy stands for the azoxy intermediate.

present reaction conditions (Table 2, entries 10–12). In addition, no conversion was found in the presence of the Au-free TiO_2 catalyst under identical conditions (Table 2, entry 9), illustrating that the presence of gold was indispensable for high catalytic activity of the title reaction.

The distinct advantages of Au/TiO_2 prompted us to investigate this system in more detail. It is noteworthy that the moderate selectivity for *m*-NA (up to 66%) is maintained at up to 98% conversion of *m*-DNB within 1 hour with Au-M/TiO_2 (Table S2†). To improve the yield of the target product, screening of the reaction conditions was then carried out. Firstly, studies on the nature of the solvent revealed that ethanol was the solvent of choice (Table S2†). When the solvent was changed to CH_2Cl_2, toluene, or dioxane, the conversion of *m*-DNB decreased to 29%, 40%, and 31%, respectively. Subsequently, the effect of hydrogen pressure on the hydrogenation of *m*-DNB was tested at 60 °C (Table S3†). With increasing hydrogen pressure from 1 to 4 MPa at 60 °C, only a marginal advance of selectivity for *m*-NA from 59 to 67% was attained. Further investigation on the effect of the reaction temperature at 3 MPa revealed that the rates of the hydrogenation could be greatly accelerated at higher temperatures (from 40 to 80 °C), as in the case of hydrogen pressure, temperature did not affect selectivity much but affected the reaction rate (Table S3†). The reaction conditions with 0.5 mol% of Au/TiO_2 at 60 °C under 3 MPa H_2 were used for further optimization studies.

Bearing in mind that the particle size has proven especially influential for supported gold catalysts,[18] we initiated a systematic study of a set of TiO_2 supported Au samples with varied mean Au particle sizes ranging from *ca.* 2 to 10 nm. Consistent with most of the previous work on Au-catalyzed hydrogenation reactions,[19] a prominent size-dependent behavior has been identified for *m*-DNB conversion over these catalysts (Fig. 5). The reaction profiles (Fig. 6) for three representative Au-1.8/TiO_2, Au-3.9/TiO_2 and Au-7.5/TiO_2 samples showed that the hydrogenation of *m*-DNB occurred through a step-wise process *via* intermediacy of *m*-nitrosonitrobenzene (*m*-NNB). While no significant formation of other intermediates has been detected as a result of experimental limitations, a closer comparison of the corresponding reaction kinetics indicates a rapid attenuation of the *m*-DNB conversion rates with increasing Au particle size. The most interesting aspect, however, is that significant *m*-NA selectivity enhancement could be achieved with the catalysts containing a relatively larger mean Au particle size (>5 nm). Among them, the best performing catalyst, Au-7.5/TiO_2, produces the maximum yield (97%) of *m*-NA within 4.5 hours. This result is remarkable, and becomes more relevant as the catalyst is applicable for a gram-scale reaction of *m*-DNB (20 mmol scale up) for 76 h, where 98% yield of *m*-NA was obtained (Scheme S1†). Under these conditions, an exceptionally high initial TOF value of 385 h^{-1} was calculated. This value compares favorably with 238 h^{-1} reported recently on an Au/TiO_2 catalyst prepared by simple impregnation for the gas phase hydrogenation of *m*-DNB (reaction at 200 °C).[8f]

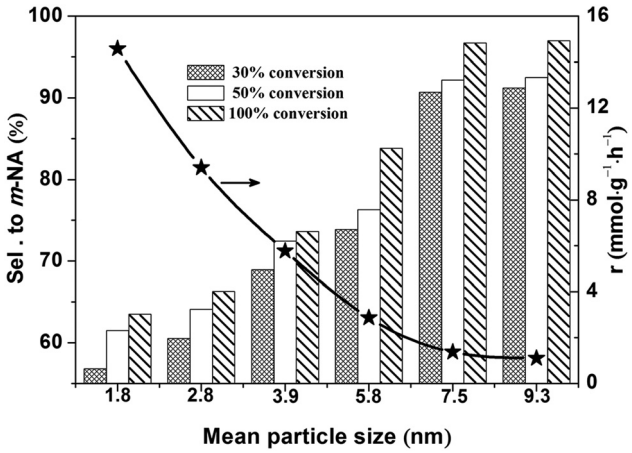

Fig. 5 Effect of the particle size in hydrogenation of *m*-DNB with various Au/TiO_2 catalysts. Reaction conditions: 0.5 mmol *m*-DNB, 0.5 mol% Au, 5 mL ethanol, 3 MPa H_2, 60 °C.

The outstanding catalytic efficiency for *m*-DNB monohydrogenation under the above mentioned test conditions over the

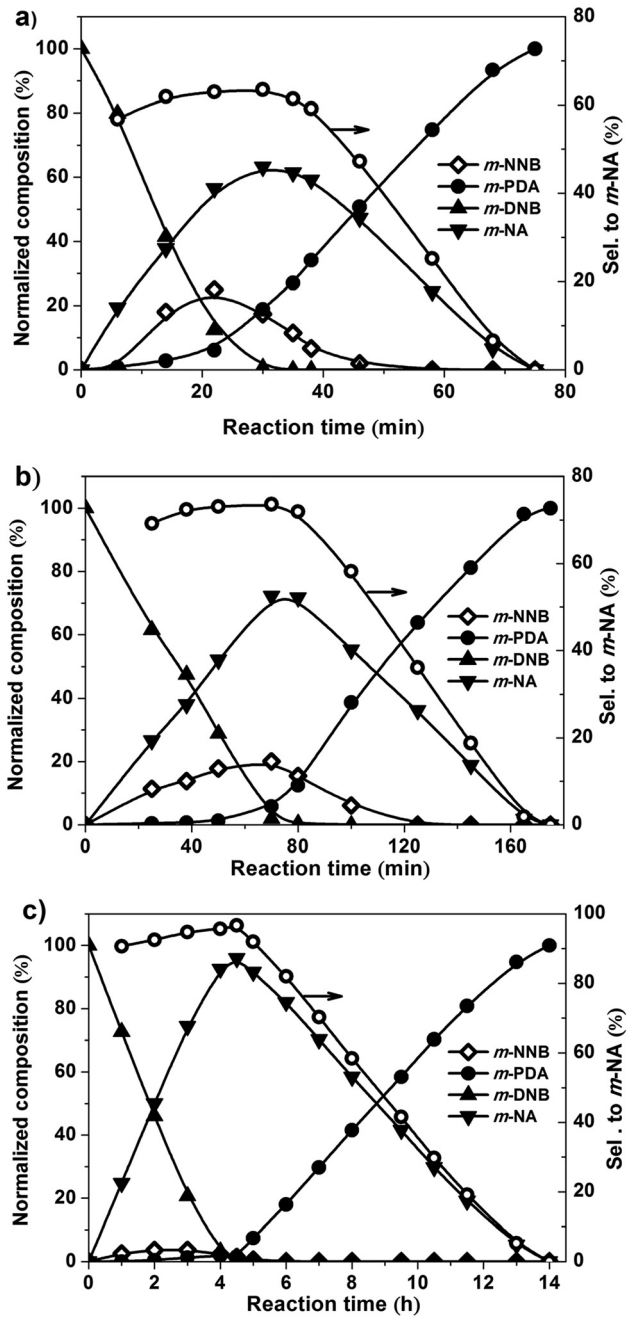

Fig. 6 Time course of the hydrogenation of *m*-DNB over (a) Au-1.8/TiO_2, (b) Au-3.9/TiO_2, (c) Au-7.5/TiO_2. Reaction conditions: 0.5 mmol *m*-DNB, 0.5 mol% Au, 5 mL ethanol, 3 MPa H_2, 60 °C.

Au-7.5/TiO_2 catalyst clearly reflects a delicate balance between the various kinetic rates associated with the title reaction. Very recently, on investigating the effect of Au particle size on gas phase *m*-DNB hydrogenation over a series of Au/TiO_2 catalysts prepared by a simple impregnation method, Keane *et al*. disclosed that the dependence of hydrogenation performance on the Au particle size can be accounted for by the resulting electronic modification of the Au particles, which is suggestive of having a strong impact on *m*-DNB adsorption/activation.[8f] To better understand the essential role of the Au particle size in

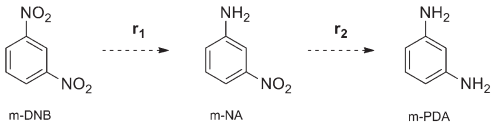

Scheme 2 Simplified reaction scheme for hydrogenation of *m*-DNB.

the present study, specific activities r_1 and r_2 were respectively measured using *m*-DNB and *m*-NA as reactants over these samples. Shown in Scheme 2 is the simplified reaction pathway involving two sequential steps for *m*-DNB hydrogenation. As shown in Fig. 7, a good correlation is observed between the specific activity ratio r_1/r_2 and the Au particle size. It should be stressed that, r_1/r_2 varies between different particle sizes. The highest value of r_1/r_2, corresponding to the highest *m*-NA selectivity, is achieved with the largest Au particle size catalyst, consistent with the superior selectivity as found for larger Au particles with respect to smaller ones. These results are consistent with a dependence of selectivity on the gold particle size as shown in Fig. 5. Taken together, it appears that the Au-7.5/TiO_2 catalyst can substantially facilitate the cumulative formation of *m*-NA relative to that of *m*-PDA, presumably *via* a preferential *m*-DNB adsorption/activation relative to other reaction intermediates, which appears to be the key factor for achieving the superior selectivity for *m*-NA in this reaction.

As stability is critical for the efficient use of any catalyst, the reusability of the Au-7.5/TiO_2 sample was investigated in the hydrogenation of *m*-DNB. After the first hydrogenation was complete, the crude reaction mixture was allowed to settle and the supernatant clear product mixture was removed from the reactor. A fresh charge of reactants was added to the catalyst residue retained in the reactor and the subsequent run was continued. This procedure was followed for four subsequent runs and the results are shown in Fig. 8. Our Au-7.5/TiO_2 catalyst showed almost the same selectivity with slight decrease in

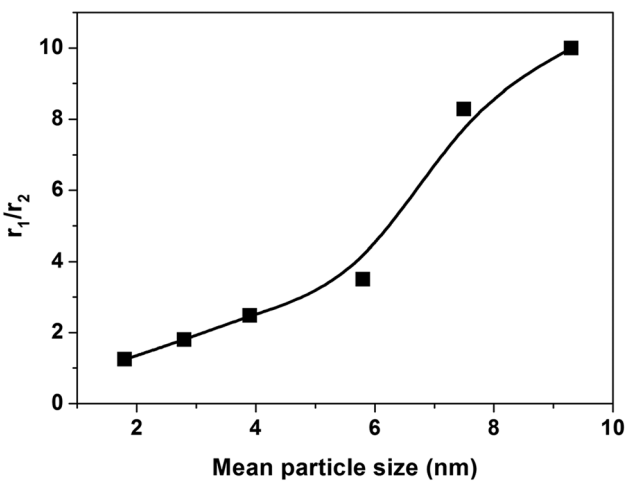

Fig. 7 r_1/r_2 as a function of the mean particle size. r_1: the reaction rate of product (*m*-NA) accumulation; r_2: the reaction rate of by-product (*m*-PDA) generation. Reaction conditions: 0.5 mmol *m*-DNB, 0.5 mmol *m*-NA, 0.5 mol% Au, 5 mL ethanol, 3 MPa H_2, 60 °C.

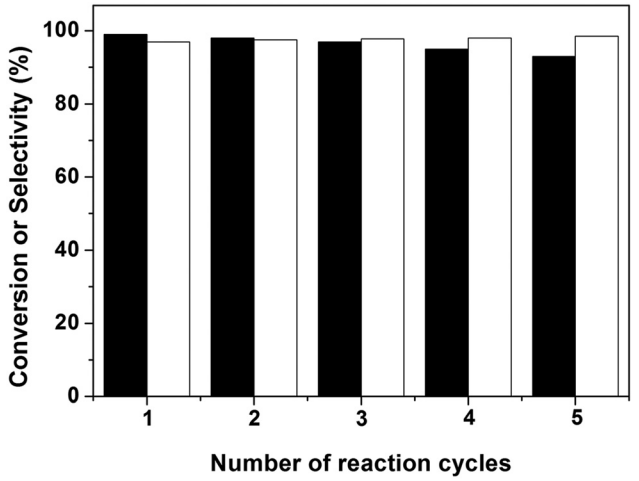

Fig. 8 Recycling of the catalyst for the synthesis of *m*-NA from *m*-DNB. Reaction conditions: 0.5 mmol *m*-DNB, Au-7.5/TiO_2 (0.5 mol% Au with respect to *m*-DNB), 5 mL ethanol, 3 MPa H_2, 60 °C, 4.5 h. (■) conversion of *m*-DNB, (□) selectivity to *m*-NA.

conversion for *m*-DNB mono-hydrogenation even after the fourth recycle. Inductively coupled plasma (ICP-AES) analysis showed the absence of Au species in the filtrate after the reaction (detection limit: <7 ppb), confirming that no leaching occurred during the reaction. XPS results (Fig. S2†) show no obvious changes in the metallic state of Au after the above successive runs. Moreover, TEM images of Au-7.5/TiO_2 after the reuse (Fig. S1†) showed that no aggregation of Au NPs occurred, and the average diameters, as well as size distributions of the Au NPs, were similar to those of the fresh one, supporting the durability of Au-7.5/TiO_2 in the recycling experiments.

Building upon these results, we started to extend this novel Au-based liquid hydrogenation protocol to a diverse range of structural dinitrobenzene derivatives. As depicted in Table 3, the reaction proceeds successfully and was remarkably selective for the synthesis of a variety of corresponding nitroanilines, regardless of the electron-withdrawing or electron-donating character of the groups attached to the aromatic rings, indicating the wide scope and synthetic utility of this catalytic system. The benefits of this catalytic process are more evident when other easily reducible groups are present in the dinitrobenzenes. For instance, the preferential formation of desired nitroanilines with selectivity over 90% and at conversion levels above 90% is observed when the nitrile or halide functional groups are included within the reactants (Table 3, entries 6, 7, 10), whereas the hydrogenation of these easily reducible groups is avoided. In fact, the selective mono-reduction of dinitrobenzene derivatives is practically independent of the position of the substitutions within the reactants, as can be seen by comparing the yields of nitroanilines when the NH_2, CH_3 or a halide group is bonded to the different position of the aromatic ring for dinitrobenzenes (Table 3, entries 4–9). More interestingly, as the complexity of the process notably increases in the case of dinitrobenzene compounds substituted with other functional groups, it is worth noting that 2,4-dinitrobenzene derivatives might produce two isomeric partially hydrogenated products, but still exhibited excellent selectivities for their mono-reduction derivatives (Table 3, entries 5, 6, 8).

Table 3 Selective monoreduction of dinitrobenzene derivatives affording the corresponding nitroanilines over Au-7.5/TiO_2[a]

Entry	Substance	Product	*t* [h]	Conv.[b] [%]	Sel.[b] [%]
1	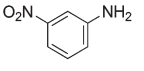	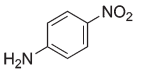	4.5	99	97
2	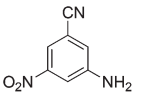	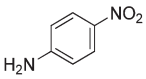	2.5	>99	96
3[c]	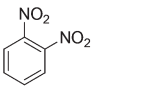	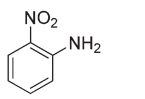	7.5	99	83
4	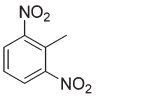	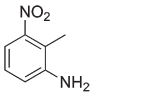	2.5	98	93
5	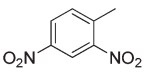	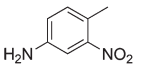	4.5	97	83[e]
		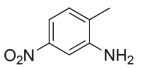			98[d] 15[e]
6	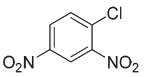	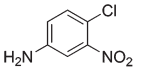	3.5	98	72[e]
		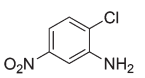			96[d] 24[e]
7	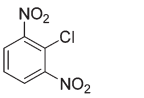	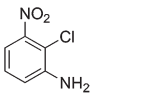	2.5	97	93
8	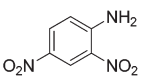	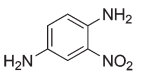	9.5	>99	89[e]
		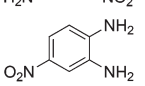			99[d] 10[e]
9	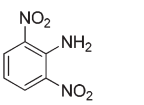	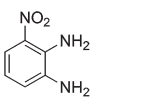	8.0	99	94
10	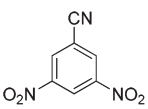	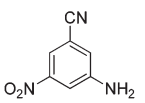	5.5	99	95

[a] Reaction conditions: substrate (0.5 mmol), 0.5 mol% Au, 5 mL ethanol, 3 MPa H_2, 60 °C. [b] Conversion and selectivity were determined by GC using *n*-dodecane as the internal standard. [c] 5 mL toluene. [d] Total selectivity of nitroanilines. [e] Ratio of two partially hydrogenated isomers.

Conclusions

Titania supported gold catalysts were applied to the mono-hydrogenation of *m*-DNB to *m*-NA in the liquid phase. Investi-

gation of recovery and reuse of the gold catalysts in the *m*-DNB reduction reaction, and careful microstructural analysis to examine the distribution and the mean particle size of supported gold NPs revealed an interesting relationship between the mean gold particle size and chemoselectivity. Relatively large Au NPs (5 to 10 nm) seem to be more selective for monoreduction of *m*-DNB than small NPs (<5 nm). The catalyst bearing the mean particle size of 7.5 nm showed the highest performance. A wide diversity of the functionalized dinitrobenzenes could be successfully reduced to the corresponding nitroanilines using this reduction system. The catalytic system presented here, which enables highly specific monoreduction of dinitroaromatics under exceedingly mild conditions, may contribute to the design of more efficient catalytic systems and may provide a new strategy for the development of green organic transformations through a careful choice of the support and fine turning the particle size.

Experimental

Catalyst preparations

Method A for Au/TiO_2 preparation. A modified deposition–precipitation (DP) procedure has been performed for the preparation of the Au-1.8/TiO_2 catalyst as follows: briefly, 1.0 g TiO_2 (Degussa P25, specific surface area: 45 $m^2\ g^{-1}$, nonporous 70% anatase and 30% rutile, purity >99.5%) was added to 100 mL of an appropriate amount of aqueous solution of $HAuCl_4$ at a fixed pH = 8 by adjusting with 0.2 M NaOH. The mixture was aged for 2 h at 80 °C under vigorous stirring, after which the suspension was cooled to room temperature. Extensive washing with deionized water was then followed until it was free of chloride ions. The samples were dried under vacuum at room temperature for 12 h before calcination at 300 °C for 4 h.

Method B for Au/TiO_2 preparation. In a typical colloidal deposition (CD) preparation, to the aqueous solution of $HAuCl_4$, an appropriate amount of PVA was added using a mass ratio Au–PVA of 1.5 : 1 at 25 °C under vigorous stirring. The obtained solution was then stirred vigorously for 10 min. A subsequent rapid injection of an aqueous solution of $NaBH_4$ (0.1 M, with molar ratio Au–$NaBH_4$ of 1 : 5) resulted in the colour of the reaction mixture immediately turning from pale yellow to dark brown, indicating the formation of Au NPs. The TiO_2 support was then added to the colloidal gold solution under stirring for 6 h. After that the solid was washed thoroughly with deionized water and dried under vacuum at 25 °C overnight. Finally, the samples were calcined at 450 °C or 500 °C for 4 h in static air. The thus obtained catalysts were denoted as Au-3.9/TiO_2 and Au-5.8/TiO_2, respectively. On the other hand, the Au-7.5/TiO_2 and Au-9.3/TiO_2 catalysts with a relatively larger mean Au particle size have been prepared according to the well-known citrate-reduction procedure: 0.5 g TiO_2 was added to 106 mL of 2.2 mM sodium citrate and was boiled under reflux with vigorous stirring, then an appropriate amount of aqueous solution of $HAuCl_4$ was quickly added to the boiling sodium citrate suspensions and boiled under reflux for 2 h, a colour change was observed, suspension initially white turned amaranth. Then, the solid was washed thoroughly with deionized water and air-dried at 65 °C for 16 h. Subsequently, it was calcined either at 500 °C or 550 °C for 4 h in static air, the thus obtained catalysts were denoted as Au-7.5/TiO_2 and Au-9.3/TiO_2, respectively.

Catalyst characterization

Elemental analysis. The Au loading of the catalysts was measured by inductively coupled plasma atomic emission spectroscopy (ICP-AES) using a Thermo Electron IRIS Intrepid II XSP spectrometer. The detection limit for Au is 7 ppb.

X-ray diffraction (XRD). The crystal structures of meso-structured CeO_2 were characterized with powder X-ray diffraction (XRD) on a Bruker D8 Advance X-ray diffractometer using the Ni-filtered Cu Kα radiation source at 40 kV and 40 mA.

Transmission electron microscopy (TEM). TEM images for the supported gold catalysts were taken with a JEOL 2011 electron microscope operating at 200 kV. Before being transferred into the TEM chamber, the samples dispersed with ethanol and deposited onto a carbon-coated copper grid and then quickly moved into the vacuum evaporator. The size distribution of the metal nano-clusters was determined by measuring about 200 random particles on the images.

UV-vis diffuse reflectance (UV-vis DRS). The sample powders were packed into a round cell with quartz window. UV/VIS-DRS measurements were performed by a Cary 400 spectrometer (Varian) equipped with a praying mantis diffuse reflectance accessory (Harrick) using $BaSO_4$ as a reference.

X-ray photoelectron spectroscopy (XPS). XPS data were re-corded with a Perkin Elmer PHI 5000C system equipped with a hemispherical electron energy analyzer. The spectrometer was operated at 15 kV and 20 mA, and a magnesium anode (Mg Kα, $h\nu$ = 1253.6 eV) was used. The C 1s line (284.6 eV) was used as the reference to calibrate the binding energies (BE).

Catalytic activity test

General procedure for the liquid phase reduction of *m*-DNB compounds. The mixture of *m*-DNB (0.5 mmol), appropriate amounts of catalysts (Au: 0.5 mol%), ethanol (5 mL) and *n*-dodecane (10 μL) as the internal standard was put into the reactor. It was purged with H_2 for five times and then H_2 was introduced to the desired pressure. The reaction temperature was maintained by a thermostat under continuous stirring of 800 rpm. For kinetic studies changes in hydrogen pressure (1 to 4 MPa) and temperature (40 to 100 °C) were made. Liquid samples were taken periodically from the reactor; *m*-DNB conversion and product selectivity were determined by a GC-17A gas chromatograph equipped with a HP-5 column (30 m × 0.25 mm) and a flame ionization detector (FID) using *n*-decane as an internal standard. Reactants and products were identified by comparison with samples, and GC–MS coupling.

Acknowledgements

Financial support by the National Natural Science Foundation of China (21273044), the Research Fund for the Doctoral Program of Higher Education (2012007000011) and Science & Technology Commission of Shanghai Municipality (08DZ2270 500 and 12ZR1401500) is kindly acknowledged.

Notes and references

1 (*a*) W. Herbst and K. Hunger, *Industrial Organic Pigments: Production, Properties, Applications*, Wiley-VCH, Weinheim, 3rd rev. edn, 2004, p. 185; (*b*) R. V. Jagadeesh, A.-E. Surkus, H. Junge, M.-M. Pohl, J. Radnik, J. Rabeah, H. M. Huan, V. Schünemann, A. Brückner and M. Beller, *Science*, 2013, **342**, 1073; (*c*) G. Wienhöfer, I. Sorribes, A. Boddien, F. Westerhaus, K. Junge, H. Junge, R. Llusar and M. Beller, *J. Am. Chem. Soc.*, 2011, **133**, 12875; (*d*) H. U. Blaser, H. Steiner and M. Studer, *ChemCatChem*, 2009, **1**, 210; (*e*) F. Visentin, G. Puxty, O. M. Kut and K. Hungerbühler, *Ind. Eng. Chem. Res.*, 2006, **45**, 4544; (*f*) G. Neri, M. G. Musolino, L. Bonaccorsi, A. Donato, L. Mercadante and S. Galvagno, *Ind. Eng. Chem. Res.*, 1997, **36**, 3619; (*g*) R. S. Downing, P. J. Kunkeler and H. van Bekkum, *Catal. Today*, 1997, **37**, 121.

2 R. J. Rahaim and R. E. Maleczka, *Synthesis*, 2006, 3316.

3 C. Qian, J. Q. Liu and X. Z. Chen, *Synth. Commun.*, 2008, **38**, 2782.

4 (*a*) D. P. He, H. Shi, Y. Wu and B. Q. Xu, *Green Chem.*, 2007, **9**, 849; (*b*) M. M. Telkar, J. M. Nadgeri, C. V. Rode and R. V. Chaudhari, *Appl. Catal., A*, 2005, **295**, 23; (*c*) G. Neria, M. G. Musolino, C. Milone, D. Pietropaolo and S. Galvagno, *Appl. Catal., A*, 2001, **208**, 307; (*d*) F. Cárdenas-Lizana and M. A. Keane, *J. Mater. Sci.*, 2013, **48**, 543; (*e*) A. Corma, P. Concepción and P. Serna, *Angew. Chem., Int. Ed.*, 2007, **46**, 7266.

5 (*a*) K. R. Westerterp, E. J. Molga and K. B. van Gelder, *Chem. Eng. Process.*, 1997, **36**, 17; (*b*) D. S. Wulfman and C. F. Cooper, *Synthesis*, 1978, 924; (*c*) R. A. Sheldon and H. van Bekkum, *Fine Chemicals through Heterogeneous Catalysis*, Wiley-VCH, Weinheim, Germany, 2001, p. 389.

6 (*a*) V. Dubois and G. Jannes, *Appl. Catal., A*, 2013, **468**, 459; (*b*) P. K. Dornan, K. G. M. Kou, K. N. Houk and V. M. Dong, *J. Am. Chem. Soc.*, 2014, **136**, 291; (*c*) G. Vilé, B. Bridier, J. Wichert and J. Pérez-Ramírez, *Angew. Chem., Int. Ed.*, 2012, **51**, 8620; (*d*) L. Huang, P. F. Luo, W. G. Pei, X. Y. Liu, Y. Wang, J. Wang, W. H. Xing and J. Huang, *Adv. Synth. Catal.*, 2012, **354**, 2689.

7 (*a*) V. M. Belousov, T. A. Palchevskaya and L. V. Bogutskaya, *React. Kinet. Catal. Lett.*, 1988, **36**, 369; (*b*) K. Gramtiko, *Izv. Khim.*, 1983, **16**, 70.

8 (*a*) S. L. Zhao, H. D. Liang and Y. F. Zhou, *Catal. Commun.*, 2007, **8**, 1305; (*b*) J. Hou, Y. H. Ma, Y. H. Li, F. Guo and L. H. Lu, *Chem. Lett.*, 2008, **37**, 974; (*c*) F. Cárdenas-Lizana, S. Gómez-Quero, N. Perret and M. A. Keane, *Catal. Sci. Technol.*, 2011, **1**, 652; (*d*) F. Cárdenas-Lizana, S. Gómez-Quero, C. J. Baddeley and M. A. Keane, *Appl. Catal., A*, 2010, **387**, 155; (*e*) F. Cárdenas-Lizana, S. Gómez-Quero and M. A. Keane, *Catal. Lett.*, 2009, **127**, 25; (*f*) F. Cárdenas-Lizana, S. Gómez-Quero, H. Idriss and M. A. Keane, *J. Catal.*, 2009, **268**, 223.

9 (*a*) G. Richner, J. A. van Bokhoven, Y.-M. Neuhold, M. Makosch and K. Hungerbühler, *Phys. Chem. Chem. Phys.*, 2011, **13**, 12463; (*b*) F. Cárdenas-Lizana, D. Lamey, N. Perret, S. Gómez-Quero, L. Kiwi-Minsker and M. A. Keane, *Catal. Commun.*, 2012, **21**, 46.

10 (*a*) A. Corma and P. Serna, *Science*, 2006, **313**, 332; (*b*) A. Corma, C. González-Arellano, M. Iglesias and F. Sánchez, *Appl. Catal., A*, 2009, **356**, 99; (*c*) A. Corma, P. Serna, P. Concepción and J. J. Calvino, *J. Am. Chem. Soc.*, 2008, **130**, 8748; (*d*) A. Corma, P. Serna and H. García, *J. Am. Chem. Soc.*, 2007, **129**, 6358; (*e*) A. Corma and P. Serna, *Nat. Protoc.*, 2006, **1**, 2590.

11 (*a*) L. He, L. C. Wang, H. Sun, J. Ni, Y. Cao, H. Y. He and K. N. Fan, *Angew. Chem., Int. Ed.*, 2009, **48**, 9538; (*b*) F. Z. Su, L. He, J. Ni, Y. Cao, H. Y. He and K. N. Fan, *Chem. Commun.*, 2008, 3531; (*c*) L. He, J. Ni, L. C. Wang, F. J. Yu, Y. Cao, H. Y. He and K. N. Fan, *Chem. – Eur. J.*, 2009, **15**, 11833.

12 (*a*) F. Cárdenas-Lizana, S. Gómez-Quero, N. Perret and M. A. Keane, *Gold Bull.*, 2009, **42**, 124; (*b*) J. Jia, K. Haraki, J. N. Kondo, K. Domen and K. Tamaru, *J. Phys. Chem. B*, 2000, **104**, 11153; (*c*) R. Zanella, C. Louis, S. Giorgio and R. Touroude, *J. Catal.*, 2004, **223**, 328.

13 (*a*) H. Tsunoyama, Y. M. Liu, T. Akita, N. Ichikuni, H. Sakurai, S. H. Xie and T. Tsukuda, *Catal. Surv. Asia*, 2011, **15**, 230; (*b*) H. Tsunoyama, H. Sakurai, Y. Negishi and T. Tsukuda, *J. Am. Chem. Soc.*, 2005, **127**, 9374.

14 (*a*) S. Díaz-Moreno, D. C. Koningsberger and A. Muñoz-Páez, *Nucl. Instrum. Methods Phys. Res., Sect. B*, 1997, **133**, 15; (*b*) J. Liu, *Microsc. Microanal.*, 2004, **10**, 55.

15 Q. Zhao, M. Li, J. Y. Chu, T. S. Jiang and H. B. Yin, *Appl. Surf. Sci.*, 2009, **255**, 3773.

16 (*a*) B. R. Panda and A. Chattopadhyay, *J. Nanosci. Nanotechnol.*, 2007, **7**, 1911; (*b*) X. Hu and D. J. Blackwood, *J. Electroceram.*, 2006, **16**, 593.

17 N. S. Chaubal and M. R. Sawant, *J. Mol. Catal. A: Chem.*, 2007, **261**, 232.

18 (*a*) M. Haruta, S. Tsubota, T. Kobayashi, H. Kageyama, M. J. Genet and B. Delmon, *J. Catal.*, 1993, **144**, 175; (*b*) M. Boudart, *Adv. Catal.*, 1969, **20**, 153.

19 (*a*) T. Fujitani, I. Nakamura, T. Akita, M. Okumura and M. Haruta, *Angew. Chem., Int. Ed.*, 2009, **48**, 9515; (*b*) S. H. Brodersen, U. Grønbjerg, B. Hvolbæk and J. Schiøtz, *J. Catal.*, 2011, **284**, 34; (*c*) J. A. van Bokhoven and J. T. Miller, *J. Phys. Chem. C*, 2007, **111**, 9245.